

Learning Robust Representation for Joint Grading of Ophthalmic Diseases via Adaptive Curriculum and Feature Disentanglement

Haoxuan Che^{1,3}, Haibo Jin¹, and Hao Chen^{1,2,3}

¹ Department of Computer Science and Engineering

² Department of Chemical and Biological Engineering

³ Center for Aging Science

The Hong Kong University of Science and Technology, Kowloon, Hong Kong
{hche, hjinag, jhc}@cse.ust.hk

Abstract. Diabetic retinopathy (DR) and diabetic macular edema (DME) are leading causes of permanent blindness worldwide. Designing an automatic grading system with good generalization ability for DR and DME is vital in clinical practice. However, prior works either grade DR or DME independently, without considering internal correlations between them, or grade them jointly by shared feature representation, yet ignoring potential generalization issues caused by difficult samples and data bias. Aiming to address these problems, we propose a framework for joint grading with the **d**ynamic **d**ifficulty-**a**ware **w**eighte**d** loss (DAW) and the **d**ual-**s**tream **d**is**e**ntangled **l**earning **a**rchitecture (DETACH). Inspired by curriculum learning, DAW learns from simple samples to difficult samples dynamically via measuring difficulty adaptively. DETACH separates features of grading tasks to avoid potential emphasis on the bias. With the addition of DAW and DETACH, the model learns robust disentangled feature representations to explore internal correlations between DR and DME and achieve better grading performance. Experiments on three benchmarks show the effectiveness and robustness of our framework under both the intra-dataset and cross-dataset tests.

1 Introduction

Diabetic retinopathy (DR) and diabetic macular edema (DME) are complications caused by diabetes, which are the most common leading cause of the visual loss and blindness worldwide [1]. It is vital to classify stages of DR and DME in clinical practice because treatments are more effective for those diseases at early stages, and patients could receive tailored treatments based on severity. Physicians grade DR into multiple stages according to the severity of retinopathy lesions like hemorrhages, hard and soft exudates, etc., while they classify DME into three stages via occurrences of hard exudates and the shortest distances of hard exudates to the macula center [23, 24], as shown in Fig.1.

Recently, large progress has been made by deep learning based methods on the grading of DR [3, 5, 6, 19] and DME [7, 8]. For example, He et al. [5] proposed

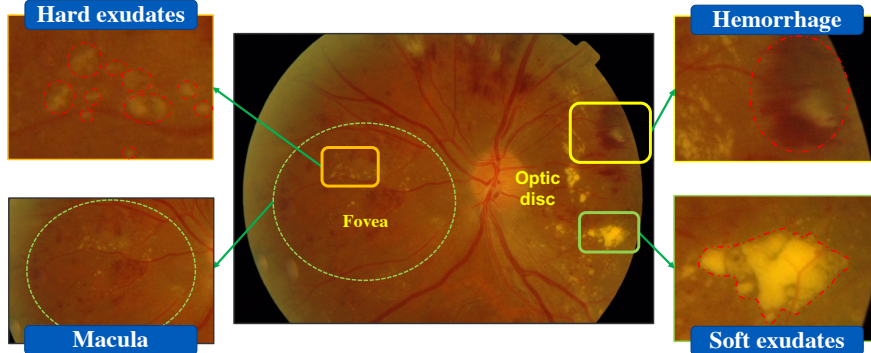


Fig. 1: Symptoms of DR and DME are different in fundus images [1, 18, 23, 24]. Physicians grade DR via soft and hard exudates, hemorrhage, etc., yet determine DME via occurrences of hard exudates and the shortest distances of hard exudates to the macula center.

a novel category attention block to explore discriminative region-wise features for each DR grade, and Ren et al. [7] presented a semi-supervised method with vector quantization for DME grading. However, DR and its associated DME were treated as separate diseases in these methods. Later, several works proposed to conduct the grading jointly [4, 9, 10]. Among them, Gulshan et al. [9], and Krasuse et al. [4] only leveraged the relationship implicitly by treating them as a multi-task problem. Subsequently, Li et al. [10] explored the internal correlation between DR and DME explicitly by designing a cross-disease attention network (CANet).

Despite the fruitful effectiveness of existing works on DR and DME joint grading, two vital issues remain unsolved. First, there is no proper solution for difficult samples, even though they have raised challenges for DR and DME grading tasks. For example, some previous works re-modify the 4-class DR grading task as a binary classification due to challenging samples [10, 31, 33]. In clinical settings, however, fine-grained grading is necessary due to the need for tailored treatments to avoid visual loss of patients. Second, the entangling feature representations are prone to emphasize the potential bias caused by the class imbalance and stereotyped disease context [32], where severe DR always accompanies DME in existing public datasets [23, 24], however, DME can occur at any stage of DR [18]. The bias can harm the generalization ability of the model, leading to subpar performance on cross-domain data. Models with robust generalization ability are especially significant for clinical application [14, 36]. However, existing works do not explore how to avoid the potential bias and mitigate the degeneration of generalization performance.

Therefore, we propose a difficulty-aware and feature disentanglement-based framework for addressing difficult samples and potential bias to jointly grade DR and DME. Firstly, inspired by curriculum learning (CL) [16], we propose the

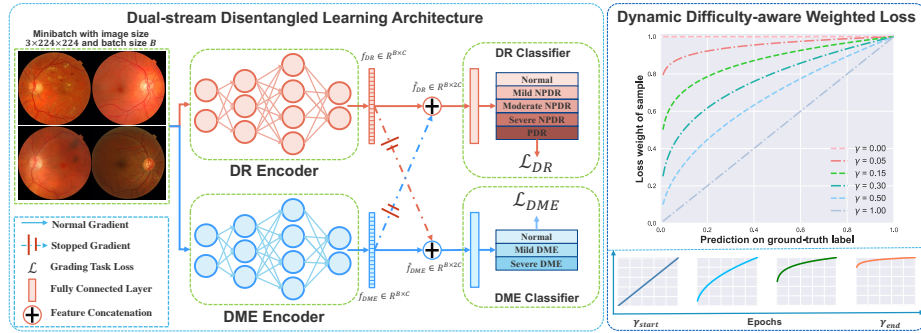


Fig. 2: The overview of our proposed framework. The framework uses two encoders to extract disentangled features f_{DR} and f_{DME} for DR and DME grading tasks, respectively. The concatenated features, \hat{f}_{DR} and \hat{f}_{DME} , flow into classifiers to learn correlations between tasks, while the model stops gradients of DR features back-propagating to the DME encoder, and vice versa. The dynamic difficulty-aware weighted loss (DAW) weights samples adaptively via predictions on true labels with γ adjusting weights dynamically during training.

dynamic difficulty-aware weighted loss (DAW) to learn robust feature representations. DAW weights samples via the evaluation of their difficulties adaptively by the consistency between model predictions and ground-truth labels. Moreover, it focuses on learning simple samples at early training, and then gradually emphasizes difficult samples, like learning curriculum from easy to challenging. Such a dynamic and adaptive curriculum helps models build robust feature representations and speed up training [16]. Meanwhile, given the success of feature disentanglement in generalization [28, 30], we design a dual-stream disentangled learning architecture (DETACH). DETACH prevents potential emphasized bias by disentangling feature representations to improve the robustness and generalization ability of models. It enables encoders to receive supervision signals only from their tasks to avoid entangling feature representations while retaining the ability to explicitly learn internal correlations of diseases for the joint grading task. Experiments show that our framework improves performance under both intra-dataset and cross-dataset tests against state-of-the-art (SOTA) approaches.

2 Methodology

An overview of our framework is shown in Fig. 2. Our framework disentangles feature representations of DR and DME via cutting off gradient back-propagation streams, and learns from simple to difficult samples via controlling the difficulty-aware parameter. In this section, we first show clues of difficult samples and generalization performance degeneration through a preliminary analysis on the Messidor dataset [24], and then introduce the proposed methods to address these issues.

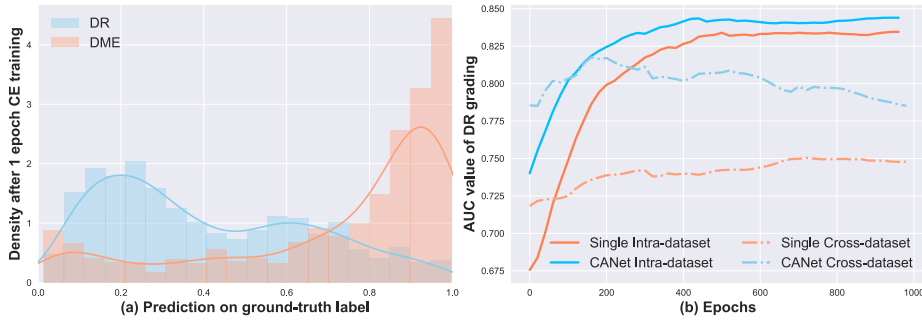


Fig. 3: Fig.(a) is a probability distribution histogram of model predictions on ground-truth labels after one epoch cross-entropy loss (CE) training, which shows divergent learning difficulties among samples and between tasks. Fig.(b) shows increasing performance in the intra-dataset test yet different trends in the cross-dataset test, implying potential emphasized bias and generalization performance degeneration.

Preliminary analysis. Fig.3(a) implies divergent difficulties among samples and between grading tasks, as also reported in [11], which claims a phenomenon of low agreement on grading for experts even adhering to a strict protocol. Such grading difficulty may be introduced by the ambiguity of samples near decision boundaries [12]. Unlike standard samples, difficult samples with ambiguity require special learning strategies [26]. Besides, as shown in Fig.3(b), an entangling representation-based model, CANet, improves its DR grading performance in the intra-dataset test yet performs continual-decreasingly in the cross-dataset test. On the contrary, a vanilla ResNet50 trained only for DR grading (denoted as Single) with cross-entropy loss (CE) improves performance in both tests. A possible explanation [28, 32] is that the model with entangled features may emphasize potential class imbalance and stereotyped correlations with DR and DME during intra-domain training, and thus suffers from performance decrease on cross-domain data. Our preliminary analysis implies the existence of difficult samples and generalization ability degeneration in DR and DME joint grading. Thus, reasonable learning strategies and disentangled feature representations are necessary for DR and DME grading.

Weighting samples via difficulty adaptively. As illustrated previously, CL can help handle difficult samples [16]. However, one critical puzzle for CL is how to measure the difficulties of samples reasonably. Instead of requiring extra models or the knowledge of experts to measure difficulty, we alternatively use consistency between model predictions and labels to evaluate the difficulties of samples for the model adaptively. It is inspired by the implicit weighting scheme of CE [15]. For notation convenience, we denote y as the one-hot encoding label of the sample, p as the softmax output of the model, and p_t as the probability of the true class where the sample belongs. We define the loss as $CE(p, y) = -\log(p_t)$

and show its gradient as:

$$\frac{\partial \text{CE}(p, y)}{\partial \theta} = -\frac{1}{p_t} \nabla_{\theta} p_t \quad (1)$$

where θ denotes parameters of the model. As Eq.1 shows, CE implicitly weights more on the samples whose model predictions are less congruent with labels, i.e., those difficult samples with smaller p_t and hence larger $1/p_t$, than samples whose model predictions are more consistent with labels, i.e., simple samples [15].

Inspired by the implicit effects of p_t on gradients of samples shown in Eq.1, we design a dynamic difficulty-adaptive weighted loss (DAW) to explicitly mitigate the enhancement on difficult samples. Specifically, we propose to add a difficulty-adaptive weight α^γ with a tunable difficulty-aware parameter $\gamma \in [0, 1]$ to CE, and we define DAW as:

$$\mathcal{L}_{DAW}(p, y, \gamma) = -\alpha^\gamma \log(p_t) \quad (2)$$

where α is the numeric value of p_t , and thus α^γ also acts on gradients directly. DAW weights samples by difficulty adaptively measured via p_t , which is continually updated during the training process. Such adaptive consideration of the keep-evolving model delivers a proper curriculum, where difficulties of samples are continual-changing for the model [13]. Moreover, DAW can emphasize or reduce the effects of p_t via controlling γ . As shown in the right of Fig.2, larger γ , i.e., more sensitive difficulty-awareness, means that the model applies smaller weights on difficult samples, and vice versa.

Learning from simple to difficult dynamically. DAW learns from simple to difficult samples by setting γ initially as γ_{start} and gradually decreasing it to γ_{end} , and the range $[\gamma_{end}, \gamma_{start}]$ denotes the dynamic difficulty-aware range. A larger γ_{start} means that the model learns less on difficult samples at the beginning, and a smaller γ_{end} means that the model treats samples more equally in the end. Such learning dynamics help the model to establish common features first, then try to learn distinctive features via its current knowledge during the training, and finally build robust feature representations [16]. After reaching γ_{end} , γ stops decreasing and the model continues to learn with $\gamma = \gamma_{end}$. In this paper, we adopt a linear decreasing strategy for γ , i.e., γ decreases equally every epoch, to verify the effectiveness of DAW in the experiment section, but more sophisticated algorithms can be used to boost the performance further.

Compared to existing CL methods, DAW handles samples adaptively and dynamically. To be specific, the existing works need extra networks or expert knowledge to evaluate the difficulty of samples as [13, 34] or sample difficulties are usually predefined and fixed during training as [16]. In contrast, for one thing, DAW uses continual-updating predictions to measure sample difficulties for the model at that moment adaptively; for another, decreasing γ focuses more on learning difficult samples than before dynamically. As a result, DAW could set a reasonable and effective curriculum for the model.

Disentangling feature representations of DR and DME. To improve the generalization ability of our model, we propose a feature disentanglement module, named **dual-stream disentangled learning architecture (DETACH)**, shown in Fig.2. It prevents the potential decrease of generalization performance by disentangling feature representations of DR and DME grading, while exploring internal correlations between DR and DME grading. Specifically, DETACH assigns two encoders with linear classifiers to DR and DME grading tasks. Encoders extract latent task features f_{DR} and f_{DME} individually. Classifiers use the concatenation of those features, denoted as \hat{f}_{DR} and \hat{f}_{DME} , for downstream DR and DME grading tasks, respectively. The core of DETACH is the feature detachment, which cuts off gradient computing of features, and thus, leads to independent back-propagation streams and disentangled features of DR and DME. For example, \hat{f}_{DR} , the concatenation of f_{DR} and detached f_{DME} , will flow into the DR classifier for grading. Thus, the DME encoder does not receive any supervision signals from the DR grading task, and vice versa. DETACH has the following strengths for DR and DME joint grading: a) encoders learn DR and DME features independently, considering different symptoms and grading criteria of DR and DME as shown in Fig.1, and b) classifiers explicitly explore internal correlations between DR and DME, and c) disentangled feature representations will prevent potential bias being emphasized by entangling feature representations [32].

3 Experiments

Datasets and implementation settings. We evaluate the proposed framework in both intra-dataset and cross-dataset tests on three fundus benchmarks: DeepDRiD [27], Messidor [24], and IDRiD [23], where the first one focuses on DR grading, and the last two have both DR and DME grading tasks. For the intra-dataset test, we split Messidor into five folds for cross-validation, and we use the train and test sets provided by the organizers for DeepDRiD and IDRiD. For the cross-dataset generalization test, we use Messidor as the train set, IDRiD as the test set, and group DR grade 3 and 4 in IDRiD as a new grade 3 to align DR severity levels with Messidor. We report the accuracy (ACC), area under the ROC curve (AUC), and macro F1-score (F1) of DR and DME grading tasks for the intra-dataset test, and additionally, report recall (REC) and precision (PRE) for the cross-dataset test. We adopt two ImageNet pre-trained ResNet50 as encoders, two fully connected layers with input size 4096 as linear classifiers for DR and DME, respectively, Adam as the optimizer, and set the initial learning rate as $1e^{-4}$, the batch size as 16, the dynamic difficulty-aware range as $[0.15, 1]$ with γ decreasing in the first 400 epochs, and the training ends at the 500th epoch.

Comparisons with state-of-the-art approaches. To the best of our knowledge, there is only one previous work [10] explicitly exploring the DR and

Table 1: Comparisons with SOTA approaches in the intra-dataset test.

Method	Messidor						IDRID					
	DME			DR			DME			DR		
	AUC	F1	ACC									
CANet [10]	90.5	66.6	89.3	84.8	61.6	71.4	87.9	66.1	78.6	78.9	42.3	57.3
Multi-task net [17]	88.7	66.0	88.8	84.7	61.7	69.4	86.1	60.3	74.8	78.0	43.9	59.2
MTMR-net [35]	89.2	64.1	89.0	84.5	60.5	70.6	84.2	61.1	79.6	79.7	45.3	60.2
Ours	92.6	70.9	90.3	86.6	61.6	70.6	89.5	72.3	82.5	84.8	49.4	59.2

Table 2: Ablation study in the intra-dataset test.

Method	Messidor						IDRID					
	DME			DR			DME			DR		
	AUC	F1	ACC									
Joint Training	90.0	64.6	88.4	84.6	59.0	69.7	84.0	61.1	75.7	82.3	41.9	57.3
DETACH w/ CE	91.7	69.7	90.1	85.5	60.2	70.7	87.7	66.1	84.3	80.2	37.9	48.5
Ours	92.6	70.9	90.3	86.6	61.6	70.6	89.5	72.3	82.5	84.8	49.4	59.2

DME joint grading. It re-modified two competitive multi-task learning methods, MTMR-Net [35] and Multi-task net [17] for the joint grading task. We compare our proposed framework with the above approaches. Note that the previous joint grading work re-modified DR grading into two categories [10], i.e., the referable and non-referable. However, we consider the original fine-grained grading problem for DR and DME. Table 1 shows the results of the intra-dataset experiment on the Messidor and IDRiD dataset. Our method consistently outperforms other SOTA approaches under the AUC metric. The results indicate that our framework learns more robust feature representations.

Ablation study. To better analyze the effects of components of our proposed method, we conduct an ablation study. Table 2 shows the result of the ablation study on Messidor and IDRiD dataset in the intra-dataset test. The joint training is an ordinary multi-task learning model containing one ResNet50 with ImageNet pre-training and two linear classifiers for DR and DME grading. The performance improves with the addition of DETACH and DAW, showing the positive effect of our proposed components. It also illustrates that the model could learn better correlations via disentangled feature representations.

The cross-dataset generalization test. A recent study suggests evaluating models in the cross-dataset test to measure generalization capacity [14]. To further investigate the generalization and robustness of our method, we conduct experiments with the above approaches in the cross-dataset test. Table 3 shows

Table 3: Comparisons and ablation study in the cross-dataset test.

Methods	DME					DR				
	AUC	F1	ACC	REC	PRE	AUC	F1	ACC	REC	PRE
CANet [10]	83.5	58.2	78.5	59.8	60.7	78.6	30.2	45.0	37.5	36.5
Multi-task net [17]	85.5	56.9	78.5	59.0	57.7	79.2	32.2	44.6	38.1	39.0
MTMR-net [35]	81.8	61.5	76.3	61.3	67.3	79.5	28.7	46.0	37.3	31.9
Joint Training	83.4	59.1	78.5	60.2	61.8	75.2	27.7	43.3	35.5	30.3
DETACH w/ CE	87.3	64.4	84.3	65.1	68.1	79.5	31.9	49.2	39.2	34.9
Ours	87.7	70.0	80.9	69.0	73.4	79.7	30.8	42.9	37.0	36.5

Table 4: Comparisons on different loss functions.

Loss	DME, IDRiD			DR, IDRiD			DR, DeepDRiD		
	AUC	F1	ACC	AUC	F1	ACC	AUC	F1	ACC
CE	84.2	64.7	79.6	76.5	47.8	57.3	83.1	51.9	61.0
FL [25]	86.2	65.4	80.6	75.3	40.5	58.3	83.2	53.0	63.0
GCE [15]	88.6	71.3	80.6	77.4	40.3	52.4	82.9	52.2	60.0
\mathcal{L}_{DAW}	90.2	74.2	83.5	82.9	50.2	55.3	84.6	52.0	60.1

the results of those approaches and ablation study under the cross-dataset test setting. The results show that our method is more robust and generalized than existing approaches. Besides, the considerable gap between the joint training and DETACH implies our disentangled learning strategy has better generalization ability than entangling feature representations.

Loss study. Finally, to verify the effectiveness of DAW, we conduct experiments comparing it with three popular loss functions, including Cross-Entropy Loss (CE), Focal Loss (FL) [25], and Generalized Cross-Entropy Loss (GCE) [15]. To avoid the influence of entangling feature representation in joint grading, we evaluate the above loss functions by individual DR or DME grading tasks on the IDRiD and DeepDRiD. We adopt a ResNet50 as the backbone and a fully connected layer with input size 2048 as the classifier, set the training epochs as 1000, and the batch size as 8. We adopt default parameter settings for the above loss functions for fairness, i.e., $\gamma = 2$ for FL, $q = 0.7$ for GCE, and dynamic difficulty-aware range $[0, 1]$ for DAW. The result in Table 4 illustrates the superiority of DAW on the grading task, where difficult samples require a reasonable learning strategy. This result also implies that DAW helps the model learn robust feature representations for grading tasks.

4 Conclusion

In this paper, we focus on the joint grading task of DR and DME, which suffers from difficult samples and potential generalization issues. To address them, we propose the dynamic difficulty-aware weighted loss (DAW) and dual-stream disentangled learning architecture (DETACH). DAW measures the difficulty of samples adaptively and learns from simple to difficult samples dynamically. DETACH builds disentangled feature representations to explicitly learn internal correlations between tasks, which avoids emphasizing potential bias and mitigates the generalization ability degeneration. We validate our methods on three benchmarks under both intra-dataset and cross-dataset tests. Potential future works include exploring the adaptation of the proposed framework in other medical applications for joint diagnosis and grading.

Acknowledgments. This work was supported by funding from Center for Aging Science, Hong Kong University of Science and Technology, and Shenzhen Science and Technology Innovation Committee (Project No. SGDX20210823103201011).

References

1. N. Cho, J. Shaw, S. Karuranga, Y. Huang, J. da Rocha Fernandes, A. Ohlogge, and B. Malanda, “Idf diabetes atlas: Global estimates of diabetes prevalence for 2017 and projections for 2045,” *Diabetes research and clinical practice*, vol. 138, pp. 271–281, 2018.
2. S. M. S. Islam, M. M. Hasan, and S. Abdullah, “Deep learning based early detection and grading of diabetic retinopathy using retinal fundus images,” *arXiv preprint arXiv:1812.10595*, 2018.
3. K. Zhou, Z. Gu, W. Liu, W. Luo, J. Cheng, S. Gao, and J. Liu, “Multi-cell multi-task convolutional neural networks for diabetic retinopathy grading,” in *2018 40th Annual International Conference of the IEEE Engineering in Medicine and Biology Society (EMBC)*. IEEE, 2018, pp. 2724–2727.
4. J. Krause, V. Gulshan, E. Rahimy, P. Karth, K. Widner, G. S. Corrado, L. Peng, and D. R. Webster, “Grader variability and the importance of reference standards for evaluating machine learning models for diabetic retinopathy,” *Ophthalmology*, vol. 125, no. 8, pp. 1264–1272, 2018.
5. A. He, T. Li, N. Li, K. Wang, and H. Fu, “Cabnet: category attention block for imbalanced diabetic retinopathy grading,” *IEEE Transactions on Medical Imaging*, vol. 40, no. 1, pp. 143–153, 2020.
6. S. Liu, L. Gong, K. Ma, and Y. Zheng, “Green: a graph residual re-ranking network for grading diabetic retinopathy,” in *International Conference on Medical Image Computing and Computer-Assisted Intervention*. Springer, 2020, pp. 585–594.
7. F. Ren, P. Cao, D. Zhao, and C. Wan, “Diabetic macular edema grading in retinal images using vector quantization and semi-supervised learning,” *Technology and Health Care*, vol. 26, no. S1, pp. 389–397, 2018.
8. A. M. Syed, M. U. Akram, T. Akram, M. Muzammal, S. Khalid, and M. A. Khan, “Fundus images-based detection and grading of macular edema using robust macula localization,” *IEEE Access*, vol. 6, pp. 58 784–58 793, 2018.

9. V. Gulshan, L. Peng, M. Coram, M. C. Stumpe, D. Wu, A. Narayanaswamy, S. Venugopalan, K. Widner, T. Madams, J. Cuadros *et al.*, “Development and validation of a deep learning algorithm for detection of diabetic retinopathy in retinal fundus photographs,” *Jama*, vol. 316, no. 22, pp. 2402–2410, 2016.
10. X. Li, X. Hu, L. Yu, L. Zhu, C.-W. Fu, and P.-A. Heng, “Canet: cross-disease attention network for joint diabetic retinopathy and diabetic macular edema grading,” *IEEE transactions on medical imaging*, vol. 39, no. 5, pp. 1483–1493, 2019.
11. C. I. Sánchez, M. Niemeijer, A. V. Dumitrescu, M. S. Suttorp-Schulten, M. D. Abramoff, and B. van Ginneken, “Evaluation of a computer-aided diagnosis system for diabetic retinopathy screening on public data,” *Investigative ophthalmology & visual science*, vol. 52, no. 7, pp. 4866–4871, 2011.
12. M. Toneva, A. Sordoni, R. T. des Combes, A. Trischler, Y. Bengio, and G. J. Gordon, “An empirical study of example forgetting during deep neural network learning,” in *International Conference on Learning Representations*, 2018.
13. L. Jiang, Z. Zhou, T. Leung, L.-J. Li, and L. Fei-Fei, “Mentornet: Learning data-driven curriculum for very deep neural networks on corrupted labels,” in *International Conference on Machine Learning*. PMLR, 2018, pp. 2304–2313.
14. R. Geirhos, J.-H. Jacobsen, C. Michaelis, R. Zemel, W. Brendel, M. Bethge, and F. A. Wichmann, “Shortcut learning in deep neural networks,” *Nature Machine Intelligence*, vol. 2, no. 11, pp. 665–673, 2020.
15. Z. Zhang and M. Sabuncu, “Generalized cross entropy loss for training deep neural networks with noisy labels,” *Advances in neural information processing systems*, vol. 31, 2018.
16. Y. Bengio, J. Louradour, R. Collobert, and J. Weston, “Curriculum learning,” in *Proceedings of the 26th annual international conference on machine learning*, 2009, pp. 41–48.
17. Q. Chen, Y. Peng, T. Keenan, S. Dharssi, E. Agro *et al.*, “A multi-task deep learning model for the classification of age-related macular degeneration,” *AMIA Summits on Translational Science Proceedings*, vol. 2019, p. 505, 2019.
18. A. Das, P. G. McGuire, and S. Rangasamy, “Diabetic macular edema: pathophysiology and novel therapeutic targets,” *Ophthalmology*, vol. 122, no. 7, pp. 1375–1394, 2015.
19. L. Tian, L. Ma, Z. Wen, S. Xie, and Y. Xu, “Learning discriminative representations for fine-grained diabetic retinopathy grading,” in *2021 International Joint Conference on Neural Networks (IJCNN)*. IEEE, 2021, pp. 1–8.
20. D. Karimi, H. Dou, S. K. Warfield, and A. Gholipour, “Deep learning with noisy labels: Exploring techniques and remedies in medical image analysis,” *Medical Image Analysis*, vol. 65, p. 101759, 2020.
21. A. Ghosh, H. Kumar, and P. Sastry, “Robust loss functions under label noise for deep neural networks,” in *Proceedings of the AAAI conference on artificial intelligence*, vol. 31, no. 1, 2017.
22. G. E. Box and D. R. Cox, “An analysis of transformations,” *Journal of the Royal Statistical Society: Series B (Methodological)*, vol. 26, no. 2, pp. 211–243, 1964.
23. P. Porwal, S. Pachade, R. Kamble, M. Kokare, G. Deshmukh, V. Sahasrabudhe, and F. Meriaudeau, “Indian diabetic retinopathy image dataset (idrid): a database for diabetic retinopathy screening research,” *Data*, vol. 3, no. 3, p. 25, 2018.
24. E. Decencière, X. Zhang, G. Cazuguel, B. Lay, B. Cochener, C. Trone, P. Gain, R. Ordonez, P. Massin, A. Erginay *et al.*, “Feedback on a publicly distributed image database: the messidor database,” *Image Analysis & Stereology*, vol. 33, no. 3, pp. 231–234, 2014.

25. T.-Y. Lin, P. Goyal, R. Girshick, K. He, and P. Dollár, “Focal loss for dense object detection,” in *Proceedings of the IEEE international conference on computer vision*, 2017, pp. 2980–2988.
26. X. Yang, M. Dong, Y. Guo, and J.-H. Xue, “Metric learning for categorical and ambiguous features: An adversarial method,” in *Joint European Conference on Machine Learning and Knowledge Discovery in Databases*. Springer, 2020, pp. 223–238.
27. DeepDRiD, “The deepdr diabetic retinopathy image dataset (deepdr) website.” <https://isbi.deepdr.org>, accessed February 20, 2022.
28. F. Träuble, E. Creager, N. Kilbertus, F. Locatello, A. Dittadi, A. Goyal, B. Schölkopf, and S. Bauer, “On disentangled representations learned from correlated data,” in *International Conference on Machine Learning*. PMLR, 2021, pp. 10 401–10 412.
29. S. Van Steenkiste, F. Locatello, J. Schmidhuber, and O. Bachem, “Are disentangled representations helpful for abstract visual reasoning?” *Advances in Neural Information Processing Systems*, vol. 32, 2019.
30. M. L. Montero, C. J. Ludwig, R. P. Costa, G. Malhotra, and J. Bowers, “The role of disentanglement in generalisation,” in *International Conference on Learning Representations*, 2020.
31. Z. Wang, Y. Yin, J. Shi, W. Fang, H. Li, and X. Wang, “Zoom-in-net: Deep mining lesions for diabetic retinopathy detection,” in *International Conference on Medical Image Computing and Computer-Assisted Intervention*. Springer, 2017, pp. 267–275.
32. S. Chu, D. Kim, and B. Han, “Learning debiased and disentangled representations for semantic segmentation,” *Advances in Neural Information Processing Systems*, vol. 34, 2021.
33. H. H. Vo and A. Verma, “New deep neural nets for fine-grained diabetic retinopathy recognition on hybrid color space,” in *2016 IEEE International Symposium on Multimedia (ISM)*. IEEE, 2016, pp. 209–215.
34. M. Kumar, B. Packer, and D. Koller, “Self-paced learning for latent variable models,” *Advances in neural information processing systems*, vol. 23, 2010.
35. L. Liu, Q. Dou, H. Chen, J. Qin, and P.-A. Heng, “Multi-task deep model with margin ranking loss for lung nodule analysis,” *IEEE transactions on medical imaging*, vol. 39, no. 3, pp. 718–728, 2019.
36. C. Chen, Q. Dou, Y. Jin, H. Chen, J. Qin, and P.-A. Heng, “Robust multimodal brain tumor segmentation via feature disentanglement and gated fusion,” in *International Conference on Medical Image Computing and Computer-Assisted Intervention*. Springer, 2019, pp. 447–456.